The Journal of Physiology

Long-chain acyl-CoA synthetase 6 regulates lipid synthesis and mitochondrial oxidative capacity in human and rat skeletal muscle

Bruno G. Teodoro[1,2], Igor H. Sampaio[1], Lucas H. M. Bomfim[3], André L. Queiroz[3], Leonardo R. Silveira[3], Anderson O. Souza[1], Anna M. A. P. Fernandes[4], Marcos N. Eberlin[4], Tai-Yu Huang[5], Donghai Zheng[5,7], P. Darrell Neufer[6,7], Ronald N. Cortright[5,6,7] and Luciane C. Alberici[1]

[1] *Department of Physics and Chemistry, Faculty of Pharmaceutical Sciences of Ribeirão Preto, University of São Paulo (USP), Ribeirão Preto, São Paulo, Brazil*
[2] *Federal Institute of Education Science and Technology of São Paulo, Sertãozinho, São Paulo, Brazil*
[3] *Department of Structural and Functional Biology, Institute of Biology*
[4] *ThoMSon Mass Spectrometry Laboratory, Institute of Chemistry, University of Campinas (UNICAMP), Campinas, São Paulo, Brazil*
[5] *Department of Kinesiology*
[6] *Department of Physiology*
[7] *East Carolina Diabetes and Obesity Institute, East Carolina University, Greenville, NC, USA*

Key points

- Long-chain acyl-CoA synthetase 6 (ACSL6) mRNA is present in human and rat skeletal muscle, and is modulated by nutritional status: exercise and fasting decrease ACSL6 mRNA, whereas acute lipid ingestion increase its expression.
- ACSL6 genic inhibition in rat primary myotubes decreased lipid accumulation, as well as activated the higher mitochondrial oxidative capacity programme and fatty acid oxidation through the AMPK/PGC1-α pathway.
- ACSL6 overexpression in human primary myotubes increased phospholipid species and decreased oxidative metabolism.

Abstract Long-chain acyl-CoA synthetases (ACSL 1 to 6) are key enzymes regulating the partitioning of acyl-CoA species toward different metabolic fates such as lipid synthesis or β-oxidation. Despite our understanding of ectopic lipid accumulation in skeletal muscle being associated with metabolic diseases such as obesity and type II diabetes, the role of specific ACSL isoforms in lipid synthesis remains unclear. In the present study, we describe for the first time the presence of ACSL6 mRNA in human skeletal muscle and the role that ACSL6 plays in lipid synthesis in both rodent and human skeletal muscle. ACSL6 mRNA was observed to be up-regulated by acute high-fat meal ingestion in both rodents and humans. In rats, we also demonstrated that fasting and chronic aerobic training negatively modulated the *ACSL6* mRNA and other genes of lipid synthesis. Similar results were obtained following ACSL6 knockdown in rat myotubes, which was associated with a decreased accumulation of TAGs and lipid droplets. Under the same knockdown condition, we further demonstrate an increase in fatty acid content, p-AMPK, mitochondrial content, mitochondrial respiratory rates and palmitate oxidation. These results were associated with increased *PGC-1α*, *UCP2* and *UCP3* mRNA and decreased reactive oxygen species production. In human myotubes, ACSL6 overexpression reduced palmitate oxidation and *PGC-1α* mRNA. In conclusion, ACSL6 drives acyl-CoA toward lipid synthesis and its down-regulation improves mitochondrial biogenesis, respiratory capacity and lipid oxidation. These outcomes are associated with the activation of the AMPK/PGC1-α pathway.

(Received 16 June 2016; accepted after revision 11 September 2016; first published online 20 September 2016)

 DOI: 10.1113/JP272962

Corresponding author L. C. Alberici: Department of Physics and Chemistry, Faculty of Pharmaceutical Sciences of Ribeirão Preto, University of São Paulo (USP). Av. Café s/n, 14040-903, Ribeirão Preto, SP, Brazil. Email: alberici@fcfrp.usp.br

Abbreviations ACSL, long-chain acyl-CoA synthetase; CCCP, carbonyl cyanide *m*-chlorophenyl hydrazone; DAG, diglyceride; DGAT, diglyceride acyltransferase; DMEM, Dulbecco's modified Eagle's medium; GFP, green fluosrescent protein; HFD, high-fat diet; LD, lipid droplet; MS, mass spectrometry; qRT-PCR, quantitative RT-PCR; siRNA, small interfering RNA; SREBP-1c, sterol regulatory element-binding protein 1c; TAG, triglyceride.

Introduction

Long-chain fatty acids are activated intracellularly by long-chain acyl-CoA synthetases (ACSL), in an ATP-dependent reaction providing acyl-CoA substrates for several metabolic pathways, including synthesis of phospholipids, diacylglycerol (DAG) and triacylglycerol (TAG), as well as protein acylation, mitochondrial β-oxidation and binding to transcription factors. The partitioning of acyl-CoA is dependent on the presence or absence of particular ACSL isoforms, their subcellular location and the tissue where they are present (Lewin *et al.* 2001; Coleman *et al.* 2002; Van Horn *et al.* 2005).

In rats, ACSL isoforms (1, 3, 4, 5 or 6) have different levels of mRNA expression based on tissue location (Mashek *et al.* 2006): (i) *ACSL1* is highly expressed in adipose tissue, liver and heart; (ii) *ACSL3* is more abundant in brain, skeletal muscle and the testis; (iii) *ACSL4* is highly expressed in liver, brain and the adrenal gland; (iv) *ACSL5* is expressed to a greater extent in liver, duodenal mucosa and brown adipose tissue; and (vi) *ACSL6* is predominately expressed in brain and skeletal muscle. The function of each ACSL isoform can also differ among tissues. For example, ACSL1 provides acyl-CoA for TAG synthesis in liver (Li *et al.* 2009) but, in skeletal muscle (Li *et al.* 2015) and heart (Ellis *et al.* 2011), these acyl-CoA products are partitioned toward mitochondrial β-oxidation.

Most of the information on how ACSL isoforms function in skeletal muscle comes from studies in rodents; comparatively, much less is understood in skeletal muscle from humans. In rats, Mashek *et al.* (2006) showed that 48 h of fasting upregulated mRNA levels of *ACSL1* and *ACSL4*, and downregulated the expression of *ACSL6*, whereas refeeding promoted the opposite effect. By contrast, the expression of *ACSL3* was not modulated by nutritional changes and the mRNA of *ACSL5* was not detected. Recently, Li *et al.* (2015) showed that the knockout of ASCL1 in mouse skeletal muscle was associated with impaired fatty acid oxidation and concomitant greater dependence on glucose metabolism. However, the role of ACSL6 in skeletal muscle remains uncharacterized.

ACSL family members not only affect fatty acid metabolism, but also play an important role in the proliferation of normal and malignant tumour cells, and regulate cell apoptosis. Dysfunction of these enzymes can lead to many metabolic diseases, such as those related to metabolic syndrome, fatty liver and neurological disorders (Yan *et al.* 2015). In humans, a defect in the activation of the fatty acids by ACSL in the muscle of black women may contribute to the maintenance of obesity (Privette *et al.* 2003).

Because of the relative sparcity of information pertaining to ACSL6 *vs.* other ACSL isoforms, and the absence of a definitive, identified function of this isoform in skeletal muscle (notably in humans), the present study aimed to refine our understanding of the function of ACSL6 in lipid partitioning toward β-oxidation or TAG synthesis. Accordingly, we used gain- or loss-of-function strategies under *in vivo* and *in vitro* conditions in both mice and humans. Given that ACSL6 expression has been reported to be downregulated by fasting, our hypothesis was that ACSL6 drives acyl-CoA toward lipid synthesis. Both rats and humans were studied to advance the existing literature and to provide novel insights into the role(s) of ACSL6 in skeletal muscle, notably for the first time in humans. These findings demonstrate that ACSL6 drives acyl-CoA toward lipid synthesis and its downregulation improves mitochondrial biogenesis, respiratory capacity and lipid oxidation.

Methods

In vivo study design with humans and ethical permission

Ethical approval. Participants provided their written informed consent prior to experiments, all of which conformed with the *Declaration of Helsinki* and were approved by the Institutional Review Board of East Carolina University (UMCIRB 12-000448).

Subject recruitment. Eleven female subjects (six lean and five obese) were recruited for the present study. Subjects were prescreened by questionnaires and personal interviews for inclusion–exclusion criteria. Subjects were all premenopausal in the early follicular phase of their menstrual cycle (days 1–4) because of the known influences of circulating sex steroids on mitochondrial function (Kane *et al.* 2011). Subjects were also sedentary (less than 30 min of physical activity per week for $>$ 6 months), non-smokers and with no history of metabolic disease (no subjects were taking medications

known to alter metabolism such as thyroid hormone replacement). Percentage body fat and fat free mass was determined by dual-energy X-ray absorptiometry (Lunar Progeny Advance; GE Healthcare Life Sciences, Little Chalfont, UK) and sedentary status was confirmed by a treadmill $\dot{V}_{O_{2peak}}$ assessment and indirect calorimetry. Height and body weight were recorded and used to calculate the body mass index (kg m^{-2}). Height and body weight were also recorded throughout the diet intervention to record possible differences in weight gain among subjects over the 7 day high-fat diet (HFD) intervention. Skeletal muscle biopsies were obtained from the lateral aspect of the vastus lateralis using a modification of the percutaneous needle biopsy technique as reported previously (Houmard *et al.* 1993).

Acute and seven day high-fat meal intervention. The diet was composed of total energy as 60% fat with remaining portions of 20% carbohydrate and 20% protein. On day 1 of the study, subjects reported to the laboratory having fasted for 10 h and were biopsied pre- and 4 h post-consumption of a high-fat liquid meal [50% daily caloric requirements; ∼70% caloric from fat at saturated: monunsaturated fatty acids: polyunsaturated fatty acids ≈ 48:37:15 provided by a mixture of Pulmocare® (Abbot Laboratories, Lake Bluff, IL, USA) and heavy cream] to allow sufficient time for lipid absorption. Following the consumption of the liquid meal and second biopsy, subjects were provided solid food by the study staff based on food preferences containing 60% total fat of the daily energy intake; 40 kcal kg^{-1} body weight. The structured solid food diet was designed to reproduce the typical Western diet with a lipid composition of 48% saturated fatty acids, 15% polyunsaturated fatty acids and 37% monunsaturated fatty acids. Established electronic protocols were used to track subject measurement and food item selection, which were monitored as macronutrient content, percentages and total energy on a daily basis for the entire study. Accordingly, subjects were trained by our study team dietician to select and measure food selections and to submit a daily electronic spreadsheet (Excel, Microsoft Corp., Redmond, WA, USA) that acted as a food calculator for the variables of interest. Daily inspection and consultation were used to provide adjustments to the subject's diet to ensure target food consumption as percentage macronutrient and total energy intake. In addition to daily contact with the subjects via email, we conducted face-to-face meetings to review dietary compliance, adjustments in food choices and replenishments of food items. On day 7, subjects were biopsied pre- and post-liquid meal as above. All diets were analysed using Nutrition Pro Software® (Axxya Systems LLC, Stafford, TX, USA) throughout and after completion of the study.

Human subject dietary compliance. The diet intervention was well tolerated by the subjects and compliance was 100.9 % ± 5.6 of target total calories, and the target of 60% of total daily calories as fat was 59% ± 1.3 (mean ± SEM).

Isolation and culture of human skeletal muscle cells

Satellite cells were isolated from 50–80 mg of fresh muscle tissues from human vastus lateralis and cultured into myoblasts as described previously (Houmard *et al.*, 1993). Briefly, tissues from biopies were transferred to ice-cold Dulbecco's modified Eagle's medium (DMEM) and all the fat and connective tissues were removed by sterilized blades and enzymatic digestion before culture into myoblasts. Myoblasts were subcultured into collegan-coated T75culture flasks in growth media containing DMEM supplemented with 10% fetal bovine serum, SkGM SingleQuot Kit (Lonza, Walkersville, MD, USA) (5 ml of BSA, 5 ml of fetuin, 0.5 ml of human epidermal growth factor, 0.5 ml of dexamethasome) and 100 U ml^{-1} Pen-Strep. Upon reaching ∼80% confluence, cells were trypsinized for subsequent transfection experiments using an Amaxa® (Lonza) electroporation technique described below.

ACSL6/green fluosrescent protein (GFP) and empty vector transfection in human skeletal muscle cells

The cells (10^6 cells per reaction) were resuspended in 100 μl of Nucleofector solution (Lonza) at room temperature combined with 4 μg of ACSL6 plasmid DNA (DNASU), whereas control cells were transfected with an empty vector plasmid DNA. The cells and plasmid DNA suspension were transfected using Amaxa Nucleofector Technology (Lonza) in accordance with the manufacturer's instructions. After transfection, the myoblasts were transferred to pre-equilibrated growth media plates at 37°C in a humidified 5% CO_2 and 95% ambient air incubator for 48 h to reach 80% confluence. Growth media was switched to differentiation media containing 2% horse-serum, 0.5 mg ml^{-1} BSA, 0.5 mg ml^{-1} fetuin and 100 U ml^{-1} Pen-Strep for the differentiation of myoblasts into myotubes. Transfection efficiency by GFP and cell viability were measured by inverted fluorescence microscopy (Olympus America Inc., Melville, NY, USA). On day 5 of differentiation, primary human myotubes were exposed to a 1:1 125 μM palmitate:125 μM oleate and then harvested on day 7 of differentiation for all cellular experiments.

In vivo study design with Wistar rats

The procedures involving rats were approved by the Institutional Ethical Commit for use of laboratory animals from the University of São Paulo – Campus of Ribeirão

Preto (Approval No. 092/2010). Male rats weighing 100 g were submitted to one of the conditions: (i) 48 h of fasting; (ii) 48 h of fasting followed by acute oral lipid ingestion of 80% saturated fat (warm butter) and 10% glucose (0.2 ml kg^{-1} body weight) by gavage (the animals were sequentially killed at 2, 4, 12 and 24 h after ingestion); (iii) an *ad libitum* diet containing 60% fat for 6 weeks; or (iv) aerobic exercise training: running at 60% of the maximum velocity capacity (determined previously by an aerobic maximum capacity test), 1 h a day, 5 days a week, for 6 weeks.

Isolation and culture of rat skeletal muscle cells

After sodium pentobarbital anaesthesia (40 mg kg^{-1}), male Wistar rats weighing 50–60 g were killed by CO_2 inhalation. Satellite cells from soleus, gastrocnemius and quadriceps muscles were quickly isolated in Dulbecco's phosphate buffered saline medium containing 1% glucose and 1% penicillin. The muscle tissue was minced and digested in DMEM containing 1.5% collagenase II, 2.5% trypsin, 0.1% DNAse and 1% penicillin at 37°C for 30 min. The trypsin was neutralized with 15 ml of prime growth medium containing 10% horse serum, 10% fetal bovine serum, 2 mM L-glutamine and 1% penicillin. The medium was centrifuged (200 g) at 4°C for 20 min and the supernatant discarded. The cells were placed in plates covered with 0.1% matrigel and cultured for 4 days.

Small interfering RNA (siRNA) transfection in rat skeletal muscle cells

The cells were transfected with specific siRNA oligo for ACSL6 (SASI_Rn01_00079210) or scrambled siRNA, obtained from Sigma-Aldrich (St Louis, MO, USA). The cell media was changed to antibiotic-free growth media containing the specific siRNA oligonucleotides (20 nM $well^{-1}$) and 0.5 μl ml^{-1} lipofectamine 2000 (Life Technologies, Grand Island, NY, USA) and maintained at 37°C with 5% CO_2 for 24 h to reach 80% confluence. Next, cell differentiation of myoblasts into myotubes was induced by 10% horse-serum (Lynge *et al.* 2001; Teodoro *et al.* 2014) for 24 h. On day 1 of differentiation, the cells were then washed with PBS and incubated with DMEM containing 10% horse-serum and 50 μM BSA-conjugated palmitate. On day 2 of differentiation, cells were trypsinized, collected, washed with PBS and suspended in the appropriate assay buffer for analyses. The mRNA content of ACSL6 after transfection was determined by a real-time quantitative RT-PCR (qRT-PCR) analysis.

Cell death assay in rat skeletal muscle cells

The cells (25×10^4) were suspended in binding buffer propidium iodide in accordance with the manufacturer's instructions (Dead Cell Apoptosis Kit; Invitrogen/Molecular Probes, Carlsbad, CA, USA). Data were acquired in a flow cytometer (Guava EasyCyte 8HP; Millipore, Hayward, CA, USA) and analysed using the accompanying software (GuavaSoft, version 2.7). Propidium iodide stains necrotic cells and cells in the later stages of apoptosis (Martin *et al.* 1995; Castedo *et al.* 2002).

Oxygen consumption monitoring in rat skeletal muscle cells

Cells were counted in a Neubauer chamber, using trypan blue to stain dead cells. The cells (10^6, 88% viability) were suspended in 2.1 ml of Krebs–Henseleit medium containing 5.6 mM glucose (pH 7.3) at 37°C and assessed for respiratory capacity using the High Resolution Oxygraph-2k system (Oroboros, Innsbruck, Austria) equipped with DataLab, version 5.0 (SDL, Pressbaum, Austria) for monitoring oxygen consumption. Oligomycin (2 μg ml^{-1}) and carbonyl cyanide *m*-chlorophenyl hydrazone (CCCP) (2 μM) were used for oxidative phosphorylation inhibition and uncoupling, respectively. The integrity of cell membrane (cell viability) during the monitoring was 85.6 $\pm$ 3.8 %, as assessed by the test of stimulatory effect of succinate plus ADP according to Pesta and Gnaiger (2012).

H_2O_2 production in rat skeletal muscle cells

Following transfection procedures, cells (5×10^5) were maintained at 37°C in 2 ml of Krebs–Henseleit medium containing 5.6 mM glucose, 2 μM Amplex ultra-red and 0.3 U ml^{-1} HRP for 40 min. An aliquot (200 μl) of medium was collected with a time course of 5 min, 20 min and 40 min. Fluorescence intensity was determined at 563/581 nm excitation/emission.

Citrate synthase activity in rat skeletal muscle cells

Cells (5×10^6 cells ml^{-1}) were frozen under liquid nitrogen and thawed twice to disrupt the mitochondria and release the citrate synthase (Siu *et al.* 2003). The homogenate was centrifuged at 12 000 $\times$ *g* at 4°C for 10 min and the supernatant containing the proteins was collected (Bharadwaj *et al.* 2015). The protein concentration was determined by Bradford assay, in a final volume of 200 μl (catalogue number 500-0006; Bio-Rad, Hercules, CA, USA). The reaction mixture contained triethanolamine-HCl buffer 0.1 M (pH 8.0), 0.3 mM acetyl-CoA, 0.5 mM oxaloacetate, 0.25% Triton X-100 and 0.1 mM 5,5′-dithiobis-2-nitrobenzoic acid. The reaction was started by the addition of 10 μg of protein. Citrate synthase activity was determined spectrophotometrically according to the method of Srere (1969).

qRT-PCR mRNA analysis

Human and rat cells (5×10^5) or tissues (~20 mg) were homogenized in TRIzol reagent (Invitrogen, Carlsbad, CA, USA) for RNA isolation. For real-time qRT-PCR analysis, RNA was reverse transcribed with IMPROM II Reverse Transcriptase (Promega, Madison, WI, USA) and used in quantitative PCR reactions containing EVA-green fluorescent dye (Bio-Rad) for rat genes and TaqMan fluorescent dye (Applied Biosystems, Foster City, CA, USA) for human genes. Relative expression of mRNAs was determined after normalization by β-actin or RPL39 for rats and 18 s for human using the $2^{-\Delta\Delta}$Ct method (Livak and Schmittgen, 2001). Quantitative PCR was performed using an Eppendorf Realplex4 Mastercycler Instrument (Eppendorf, Hamburg, Germany) for rat samples and an ABI ViiA 7 PCR System (Thermo Fisher Scientific, Waltham, MA, USA) for human samples. Rat primers used for RT-PCR were obtained from Sigma: *PGC1α* (Fw, 5′-CAAGCCAAACCAACAACTTTATCTCT-3′; Rw, 5′-CACACTTAAGGTTCGCTCAATAGT-3′), *β-actin* (Fw, 5′-CACTTTCTACAATGAGCTGCG-3′; Rw, 5′-CTGGATGGCTACGTACATGG-3′), *RPL39* (Fw, 5′-CAAAATCGTCCTATTCCTCAATGG-3′; Rw, 5′-CAGTAGAAATCCTCAGTCTGGC-3′), *UCP3* (Fw, 5′-ATGAGTTTTGCCTCCATTCG-3′; Rw, 5′-GGCGTATCATGGCTTGAAAT-3′), *UCP2* (Fw, 5′-ATGTGGTAAAGGTCCGCTTC-3′; Rw, 5′-CATTTCGGGCAACATTGGG-3′), *ACSL6* (Fw, 5′-CAGTAGAAATCCTCAGTCTGGC-3′; Rw, 5′-GGCTCACTTCGGATGTAGATG-3′), *DGAT1* (Fw, 5′-GACAGCGGTTTCAGCAATTAC-3′; Rw, 5′-GGGTCCTTCAGAAACAGAGAC-3′), *DGAT2* (Fw, 5′-ACAGTGGGTCCTATCCTTCC-3′; Rw, 5′-ATCTCCTGCCACCTTTCTTG-3′), *ACSL1* (Fw, 5′-GAAAGCCAAACCAGCCATATG-3′; Rw, 5′-GAAAAGATGCCGATGAACTGC-3′), *ACSL3* (Fw, 5′-ATGAAAACGGACAGAGGTGG-3′; Rw, 5′-TGCCTCAACTTTGCCTAGAG-3′).

Lipid droplet (LD) analyses in rat and human cells

The cells (25×10^4) were fixed with paraformaldehyde 4% for 15 min at 37°C at 5% CO_2. Under these conditions, the cells were permeabilized with PBS plus 0.1% Triton for 5 min and then incubated with 10 μg ml^{-1} BodiPy (Molecular Probes) for 30 min. The cells were then washed with PBS and read. Images were acquired in a CTR 6000 fluorescence microscope (Leica Microsystems, Wetzlar, Germany) using a 40× long objective, at 493/503 nm, and then they were quantitatively analysed using Image J (NIH, Bethesda, MD, USA).

Lipid extraction and analyses in rat and human cells

Cells (5×10^6) were homogenized in 2.25 mL of H_2O in ice, and then 2.5 ml of hexane and 1.45 ml of methanol were quickly added for lipid extraction. The lipid extracts were analysed by easy ambient sonic-spray ionization mass spectrometry (MS) in both the negative and positive ion modes (Alberici *et al.* 2011) using a single-quadrupole mass spectrometer (Shimadzu Corporation, Kyoto, Japan) equipped with a homemade easy ambient sonic-spray ionization source (Haddad *et al.* 2006; Haddad *et al.* 2008). As shown in Fig. 3*C*, the relative changes in some of the ion peaks were evaluated by plotting the ratio of the absolute abundance of the ion to that of the ion of m/z 550. This was also adopted in Fig. 3*D*, where 227 was the reference ion peak. For Fig. 6*C*, trilinolein (m/z 901 = [trilinolein+Na]$^+$) at a final concentration of 1 mM was added to the samples and used as internal standard (Fernandes *et al.* 2012). Identification of lipid structures was performed by comparing our data with that of previous studies (Brugger *et al.* 1997; Magnusson *et al.* 2008; Goto-Inoue *et al.* 2012).

Fatty acid oxidation determination in rat and human cells

Experiments utilizing [1-^{14}C]palmitate (Perkin Elmer, Boston, MA, USA) were performed to measure fatty acid oxidation in the primary human skeletal myotubes from the ACSL6 overexpression or control (empty vector) groups according to modified methods reported by Cortright *et al.* (2006). In brief, differentiated human skeletal muscle cells were incubated in sealed reaction plates at 37°C in a humidified 5% CO_2 and 95% ambient air incubator for 3 h in differentiation media containing 100 μM palmitate, 12.5 mM Hepes, 0.25% BSA, 1 mM carnitine and 10 μCi ml^{-1} [1-^{14C}] palmitate (Sigma). Following the incubation period, the reactions were terminated by the addition of 50 μl of 70% perchloric acid to the incubation wells. The incubation plate was transferred to an orbital shaker and $^{14}CO_2$ was trapped in the adjoining well in 200 μl of 1 M NaOH for 1 h. Radioactivity as $^{14}CO_2$ (complete palmitate oxidation) was determined by liquid scintillation counting using 4 ml of Uniscint BD (National Diagnostics, Atlanta, GA, USA). The remaining cell pellets from the oxidation studies were washed twice with ice-cold PBS, harvested in 200 μl 0.05% SDS, and cell lysates were stored at −80°C for subsequent protein determination and cellular lipid extraction. The rate of fatty acid oxidation was expressed as pmol μg^{-1} protein h^{-1}.

Western blotting analysis in rat and human cells

Aliquots of cell lysate (10–30 μg of protein) were separated by SDS-PAGE and transferred to a polyvinylidene fluoride membrane. Briefly, after blocking with non-fatty milk (10%), the membrane was incubated overnight at 4°C with appropriate dilutions of primary antibodies, including

p-AMPK (Cell Signaling Technology, Beverly, MA, USA), AMPK (Cell Signaling Technology), diglyceride acyltransferase (DGAT)1 (Santa Cruz Biotechnology, Santa Cruz, CA, USA), ACSL6 (Sigma) and β-actin (Cell Signaling Technology). After washing in TBST (3 × 10 min), membranes were incubated with the appropriate secondary antibody conjugated with HRP for 120 min at room temperature. Antibody binding was detected by enhanced ECL and ECL-Prime® Chemiluminescent Substrate (GE Technology, Piscataway, NJ, USA) in accordance with the manufacturer's instructions. Blot images were obtained digitally using a ChemiDoc XRS+ (Bio-Rad) system based on CCD high-resolution. β-actin or α tubulin was used to establish equality of protein loading.

Statistical analysis

Data are expressed as the mean ± SEM. For culture experiments, *n* indicates the number of different cultures obtained from different subjects. Each condition in cell culture was performed in triplicate. Statistical analysis was performed using a paired Student's *t* test for two-mean comparison (e.g. human and rat cell incubations for treatment and control derived from the same subjects) or one-way ANOVA for multiple comparisons using Prism, version 5.01 (GraphPad, San Diego, CA, USA). $P < 0.05$ was considered statistically significant as established *a priori*.

Results

ACSL6 mRNA expression under different metabolic conditions in skeletal muscle of rats and humans

Rats. Verification of *ACSL6* mRNA expression in skeletal muscle from rats was evaluated after metabolic interventions: (i) fed to fast states; (ii) aerobic exercise; and (iii) acute and chronic ingestion of a HFD. Figure 1*A* depicts a 40% decrease in *ACSL6* mRNA following the 48 h fast. This was accompanied by a decreased expression of steroyl response element binding protein 1c (*SREBP-1c*) (Fig. 1*A*), a key transcription factor that regulates cellular lipogenesis in liver, skeletal muscle and adipose tissue (Bizeau *et al.* 2003), and *DGAT1* (Fig. 1*A*), an enzyme that catalyses the conversion of DAG and acyl-CoA into TAG (Cases *et al.* 1998). After aerobic training (6 weeks, 5 days per week, once a day, 60 min at 70% of maximal aerobic capacity), *ACSL6* mRNA was reduced 35% (Fig. 1*B*). Four and 12 h after acute ingestion of a high-fat meal (80% saturated fat, 10 ml kg^{-1}), *ACSL6* mRNA was significantly higher than before ingestion (0 h, 48 h fasted) (Fig. 1*C*). This was accompanied by elevated transcription levels of SREBP-1c (Fig. 1*D*) and *DGAT1* (Fig. 1*E*). As a regulator for the transcription of several genes of lipid synthesis (Eberlé *et al.* 2004), *SREBP-1c* mRNA was found to be highly expressed 2 h before the increments in *ACSL6* and *DGAT1* expressions. After 24 h, the transcription levels of these genes were reduced, returning to the levels found during the fasting state. Surprisingly, after a chronic HFD (60% lipids, for 6 weeks), *ACSL6* mRNA expression was reduced by ∼40% (Fig. 1*F*), suggesting that this downregulation represents a defence mechanism against over accumulation of lipids in the skeletal muscle.

Humans. In fasting humans, we found that obese subjects have lower levels of *ACSL6* mRNA compared to lean subjects (Fig. 1*G*). Four hours after the high-fat meal (70% total energy as fat), *ACSL6* mRNA expression was increased 2.5 times over fasting levels in the skeletal muscle of both lean and obese. Unlike in rats, a chronic HFD(60% fat, 7 days) did not alter the transcription levels of *ACSL6* mRNA in lean subjects (Fig. 1*H*). As one explanation, these differential responses may be a result of differences in the period of HFD ingestion (1 week for humans and 4 weeks for rats). Regardless, these results suggest that ACSL6 is an important gene that is positively modulated during conditions associated with lipid synthesis in skeletal muscle of rats and humans. Given tissue mass restrictions from human participants, this was not possible.

Effects of knockdown of ACSL6 in primary cells of rat skeletal muscle

Next, we confirmed the effects of decreased expression of *ACSL6* in a culture of primary skeletal muscle cells. At 20 nM, ACSL6-specific siRNA oligo transfection of cells decreased 75% the transcription levels of ACSL6; otherwise, 40 and 80 nM decreased the transcription by ∼50% and 40%, respectively (Fig. 2*A*). These results probably represent RISC complex saturation. Thus, the remainder of experiments utilized ACSL6 siRNA at a concentration of 20 nM. It should be noted that this decrease of *ACSL6* mRNA did not alter cell viability (late apoptosis/necrosis) compared to control (scrambled siRNA transfection) but was markedly reduced compared to dimethyl sulphoxide (positive control of cell death) conditions (Fig. 2*B* and *C*).

The knockdown of *ACSL6* also reduced the accumulation of lipophilic dye BODIPY, a specific probe for high non-polar lipids (mainly TAG), as fluorescent particles in the cytoplasm of cells (Fig. 3*A*), indicating reductions in LD density (Fig. 3*B*). These results were reinforced by MS analyses, which demonstrated a significant decrease in the abundances of $[TAG+Na]^+$ ions of *m*/*z* 853 (C50:2), 855 (C50:1), 879 (C52:3), 881 (C52:2), 905 (C54:4) and 907 (C54:3) (Fig. 3*C*) in ACSL6 siRNA transfected cells compared to control cells, as well

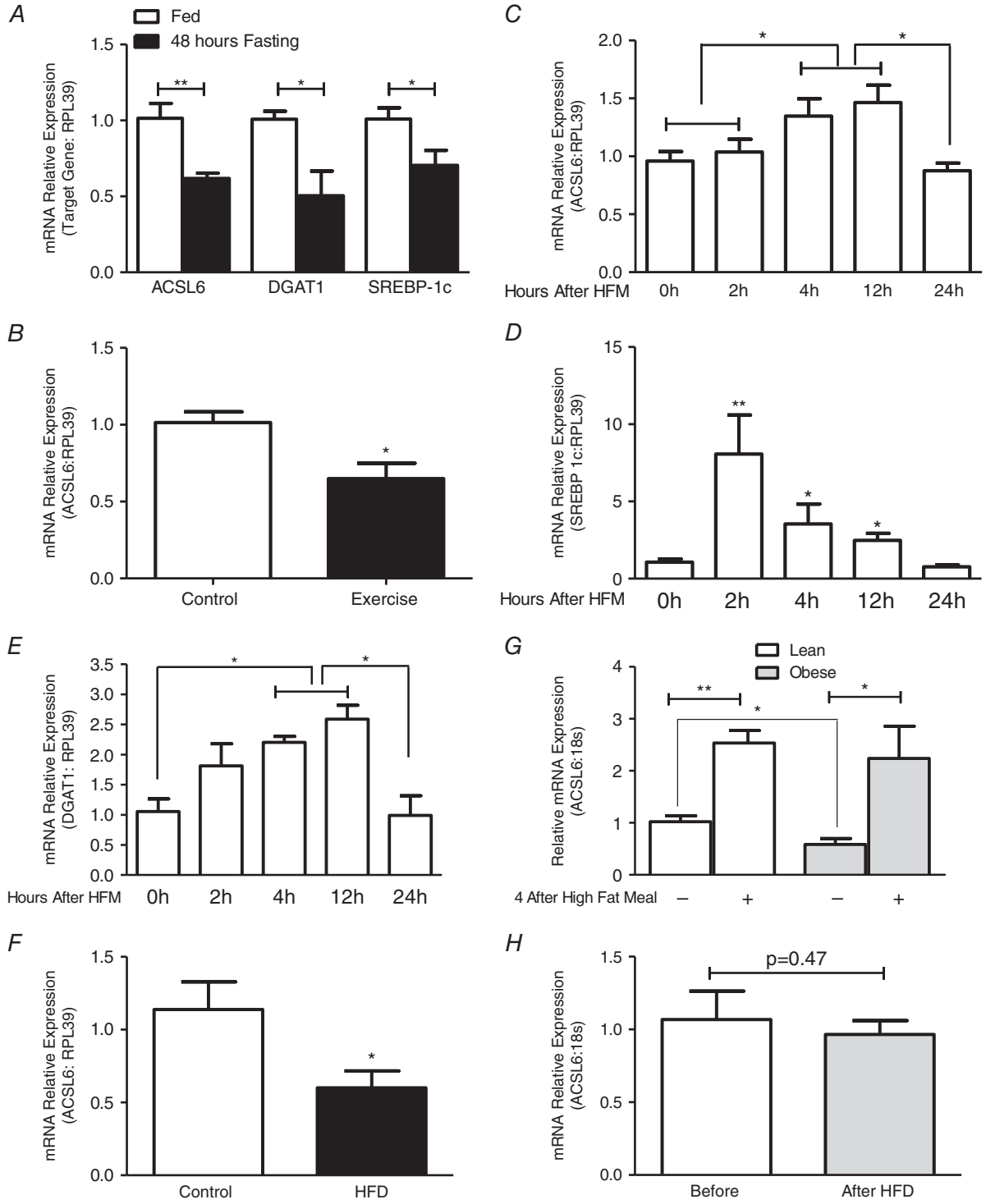

Figure 1. ACSL6, SREBP-1c and DGAT-1 mRNA expression at different metabolic conditions in skeletal muscle of rats and humans

Rat muscle ACSL6, SREBP-1c and DGAT1 mRNA expression after 48 h of fasting (*A*) ($n = 5$); ACSL6 mRNA expression after 6 weeks of aerobic exercise (*B*) ($n = 6$); ACSL6 (*C*), SREBP-1c (*D*) and DGAT1 (*E*) mRNA expression in a time course after acute lipid ingestion ($n = 5$); and ACSL6 mRNA expression after 6 weeks of a HFD (*F*) ($n = 6$). Lean and obese human muscle ACSL6 mRNA 4 h after acute ingestion of a high-fat meal (*G*) and lean human ACSL6 mRNA 7 days after ingestion of a HFD (*H*) ($n = 6$ for lean and $n = 5$ for obese). *$p < 0.05$; **$p < 0.01$.

as a decreased abundance of $[DAG+K]^+$ ion of *m/z* 685 (C38:1). Decreased $[sphingomyelin+Na]^+$ ions of *m/z* 725 (C16:0) and $[phosphatidylcholines+Na]^+$ ions of *m/z* 756 (C32:0) were also noted, although without changes in the abundances of $[phosphatidylcholines+Na]^+$ ions of *m/z* 782 (34:1) 808 (36:2) and 827 (50:5) (Fig. 3*C*). By contrast, we found increased abundances of $[FA-H]^-$ ions of *m/z* 255 (C16:0) and 283 (C18:0) (Fig. 3*D*). Concomitantly, we also observed a decrease in *DGAT1* and *SREBP-1c* mRNA (Fig. 3*E*). These results corroborate findings found *in vivo* in rats and humans, indicating that ACSL6 is involved in lipid biosynthesis in skeletal muscle that exists across mammalian species.

Effects of knockdown of ACSL6 on mitochondrial metabolism in primary cells of rat skeletal muscle

Using high resolution respirometry, we determined whether decreased *ACSL6* gene expression promotes changes in cellular respiration in non-permeabilized cells (Fig. 4*A* and *B*). The knockdown of *ACSL6* increased mitochondrial respiration rates by 25% in the ROUTINE state (State *R*), in which exogenous substrates in culture media supports respiration, whose rate depends on cellular ATP demand; 28% in non-phosphorylating or LEAK state (State *L*, with oligomycin), in which oxidative phosphorylation is inhibited and O_2 consumption reflects intrinsic uncoupling such as that caused by proton leak;

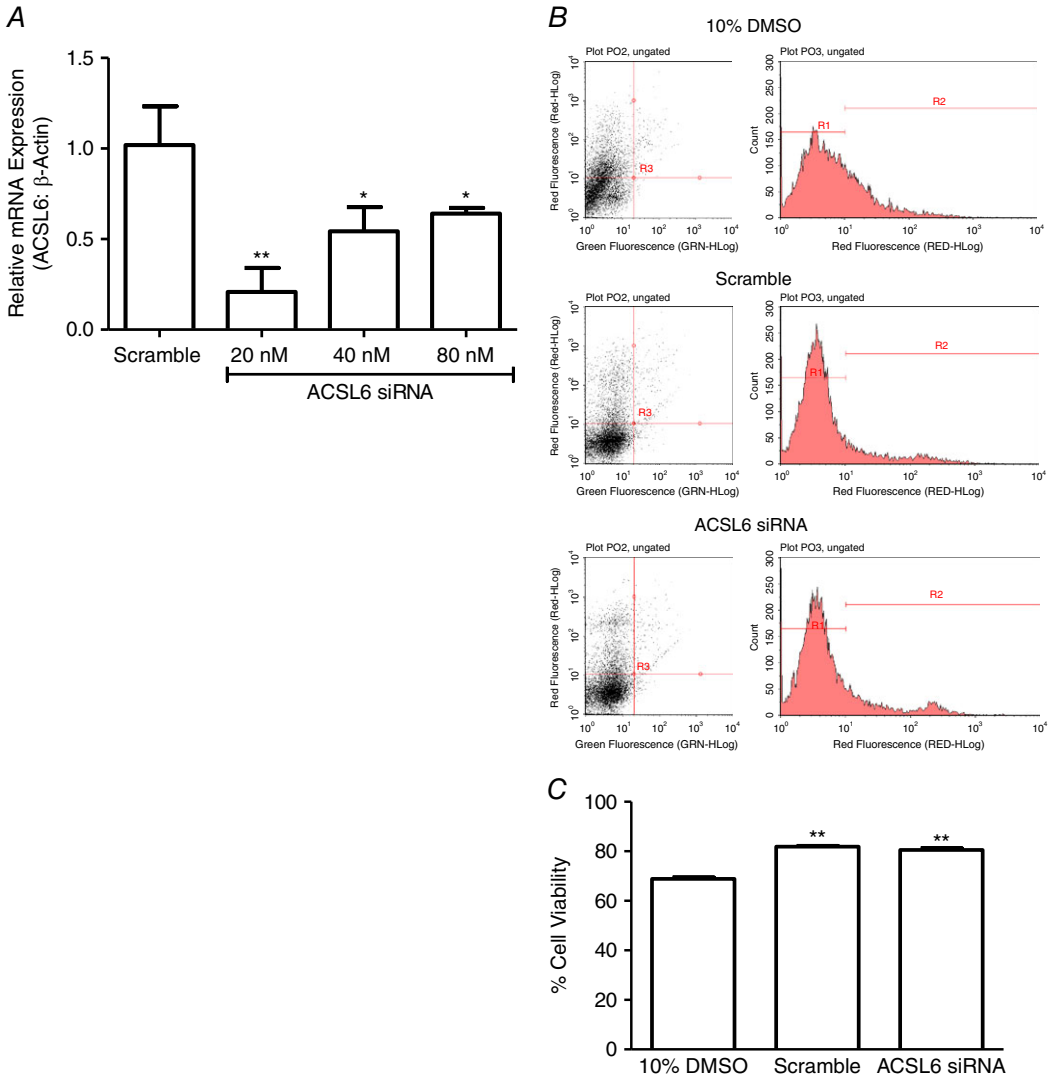

Figure 2. Effects of specific ACSL6 siRNA tritation on ACSL6 mRNA expression and cell viability in primary cells of rat skeletal muscle
ACSL6 mRNA at 20, 40 and 80 nM ACSL6 siRNA or scrambled siRNA (*A*) ($n = 6$), representative plots from flow cytometry acquisition (*B*) and percentage of cell viability (*C*) in cells at 30 nM ACSL6 siRNA, 10% dimethyl sulphoxide (necrose condition) or scramble ($n = 6$). $^*P < 0.05$; $^{**}P < 0.01$. [Colour figure can be viewed at wileyonlinelibrary.com]

and 50% in NONCOUPLED respiratory state (State *E*), in which the protonophore CCCP collapses the electrochemical H^+ potential across the inner mitochondrial membrane, and hence stimulates maximum electron transfer and respiration. Collectively, these results suggest an elevation mitochondrial respiratory capacity (content) or electron chain function (or both). In conjunction with these findings, we observed enhanced phosphorylation of AMPK, as indicated by an increased p-AMPK/AMPK ratio (demonstrating the activation of this promoter of mitochondrial biogenesis) (Fig. 4*C* and *D*), an elevated mRNA expression of peroxisome proliferator-activated receptor-γ coactivator 1 α (*PGC-1α*) (a master regulator of mitochondrial biogenesis) (Fig. 4*E*) and higher citrate synthese activity (an indicator of mitochondrial content) (Fig. 4*F*).

Moreover, the gene expression of uncoupling proteins (*UCP3* and *UCP2*) was also upregulated in *ACSL6* knockdown cells (Fig. 4*E*). These proteins promote increments in mitochondrial respiration and substrate utilization, and decrease the release of reactive oxygen species (Mailloux and Harper, 2011). Concomitant

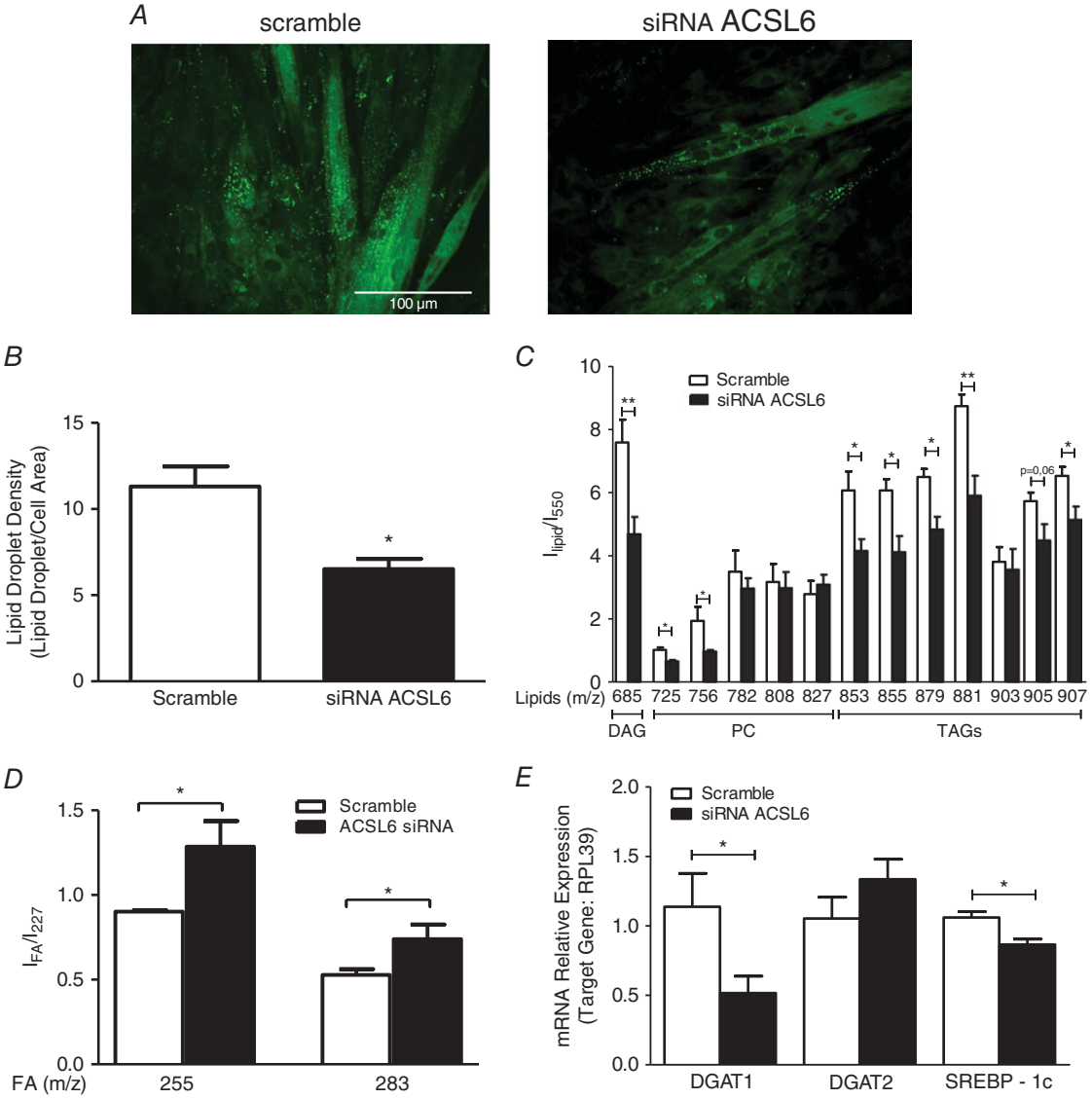

Figure 3. Effects of ACSL6 knockdown in primary cells of rat skeletal muscle
Representative fluorescence microscopy images of LD staining using BODIPY 493/503 in scramble (left) and siRNA ACSL6 transfected (right) cells (*A*) ($n = 3$ independent culture and seven images of each culture); LD density per cell (*B*); I_{LIP}/I_{550} = absolute intensity of the ion peaks of lipids/absolute intensity of the ion peak of *m/z* 550, DAG, phosphatidylcholine (PC) and TAG (*C*) ($n = 5$); and I_{LIP}/I_{227} = absolute intensity of the ion peaks of lipids/absolute intensity of the ion peak of *m/z* 227, fatty acid (FA) (*D*) ($n = 5$) analysed by MS, mRNA expression DGAT1, DGAT2 and SREBP-1c (*E*) ($n = 6$) in scramble and siRNA ACSL6 transfected cells. $^*P < 0.05$; $^{**}P < 0.01$. [Colour figure can be viewed at wileyonlinelibrary.com]

with these findings, we observed a decreased in H_2O_2 release following *ACSL6* knockdown (Fig. 4*G* and *H*). Although we did not find differences in the expression of 3-hydroxyacyl-CoA dehydrogenase (*HAD*), an enzyme of β-oxidation of fatty acids, we observed higher radioactive-labelled palmitate oxidation (15%) in cells after ACSL6 knockdown (Fig. 4*I*).

Effects of ACSL6 overexpression in primary cells of human skeletal muscle

Because the *in vivo* acute lipid ingestion increased *ACSL6* mRNA expression in human skeletal tissue (Fig. 1*G*), we next investigated the effects of ACSL6 overexpression in cultured human skeletal muscle cells. Primary myotubes were efficiently transfected (40%), as confirmed by fluorescence of GFP. Because the cells were transfected when they were in the myoblast stage, we confirmed transfection efficiency through the differentiation process in the myotubes (Fig. 5*A*). The transfected cells presented 600x greater *ACSL6* mRNA (Fig. 5*B*). Under these conditions, we observed similar TAG content, as analysed by Bodipy fluorescence (Fig. 6*A* and *B*) and MS (Fig. 6*C* and *D*), which can be related to similar DGAT1 protein expression (Fig. 6*E*). Furthermore, ACSL6 overexpression increased ion abundance by 60% for sphingomyelin and

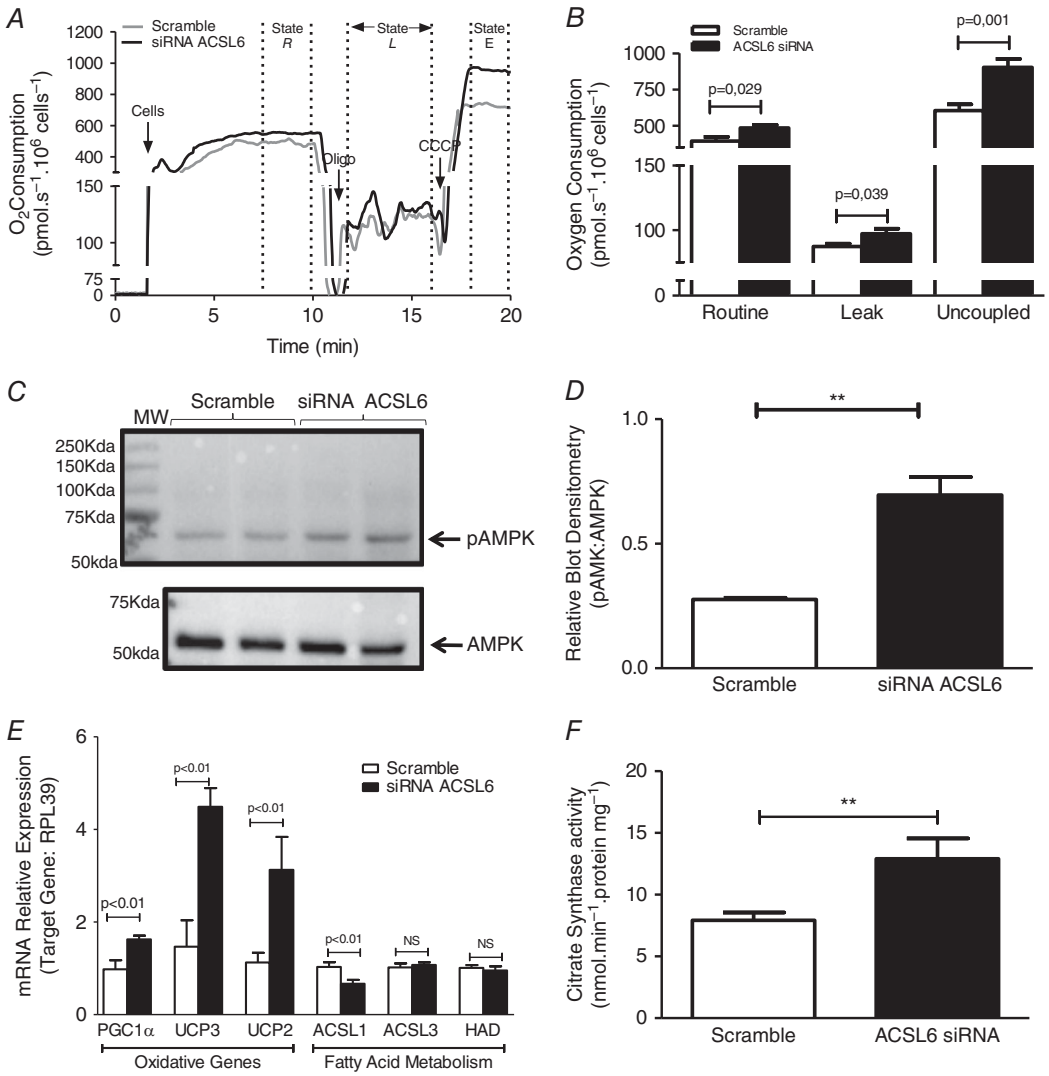

Figure 4. Effects of ACSL6 knockdown on oxidative metabolism in primary cells of rat skeletal muscle
Typical traces of O_2 consumption (*A*) and rates (pmol s^{-1} mg $protein^{-1}$) (*B*) in ROUTINE (State *R*), LEAK (State *L*) and NONCOUPLED (State *E*) states by scramble and siRNA ACSL6 transfected cells. Where indicated, cells (10^6), oligomycin (oligo, 1 μg ml^{-1}) and CCCP (2 μM) were added to the medium ($n = 12$). Immunoblotting (*C*) and blot densitometry (*D*) of p-AMPK and AMPK ($n = 4$), mRNA expression of PGC1α, UCP2, UCP3, ACSL1, ACSL3 and HAD (*E*) ($n = 6$), citrate synthase activity (*F*) ($n = 4$), time-scan (*G*) and rates (*H*) of H_2O_2 production ($n = 6$) and radiolabelled ^{c14}palmitate oxidation (*I*) ($n = 4$) in scramble and siRNA ACSL6 transfected cells.*$P < 0.05$; **$P < 0.01$.

89% for phosphatidylcholine (Fig. 6*C* and *D*), as well as reduced palmitate radio-labelled oxidation (Fig. 6*F*) and *PGC-1α* mRNA expression (Fig. 6*G*). These results indicate that ACSL6 overexpression in skeletal muscle cells from humans decreases cellular oxidative capacity. Given the reduction in *PGC-1α*, these findings further suggest a reduction in mitochondrial content, in contrast to the opposing effects observed following ACSL6 knockdown in skeletal muscle cells from rats. Moreover, ACSL6 overexpression was more effective in elevating the synthesis of phospholipids *vs.* TAG.

Discussion

In humans, the function of ACSL isoforms has been analysed in immortalized cancer cells (Parkes *et al.* 2006; Cao *et al.* 2010; Wu *et al.* 2011), tumor biopsies from prostate cancer (Fujimura *et al.* 2014) and the gut (Heimerl *et al.* 2006), where an upregulation of ACSL3 and ACSL1/ACSL4 gene expression was observed, respectively. To the best of our knowledge, there is only one study describing reduced ACSL5 mRNA expression in skeletal muscle of obese women resistant to weight loss by diet (Adamo *et al.* 2007) and no studies exist that address the function of ACSLs in human skeletal muscle. Accordingly, the present study describes for the first time that *ACSL6* gene expression is present in human skeletal muscle and is modulated *in vivo* by diet, as demonstrated by the time-course for ACSL6 upregulated expression induced by an acute high-fat meal. Given the observation of an impaired *β*-oxidative system in ACSL6-overexpressed transfected primary myotubes, the present results further indicate that the enzyme channels acyl-CoA substrate toward lipid synthesis in human skeletal muscle. Increments in TAG content following ACSL6 overexpression was not observed, although increased phosphatidylcholine species was noted. Both lipids share the same synthetic metabolic pathway, where DAG is the last common intermediate (Bosma *et al.* 2012; Bosma *et al.* 2016). Because DGAT mRNA expression was not changed under ACSL6 overexpression, we speculate that DAG is following the pathway of phosphatidylcholine synthesis. This suggests the involvement of ACSL6 also in phospholipid synthesis in skeletal muscle. These findings are supported by studies in rat brain, where it was observed to be involved in the incorporation of unsaturated fatty acids into phospholipids (Soupene *et al.* 2010; Chen *et al.* 2011).

ACSL6 function was previously only described in neuronal cells (PC12) (Marszalek *et al.* 2005) and in the brain from rats (Soupene *et al.* 2010; Chen *et al.* 2011). Consequently, we extend these initial findings using our rat model, where we further characterize the

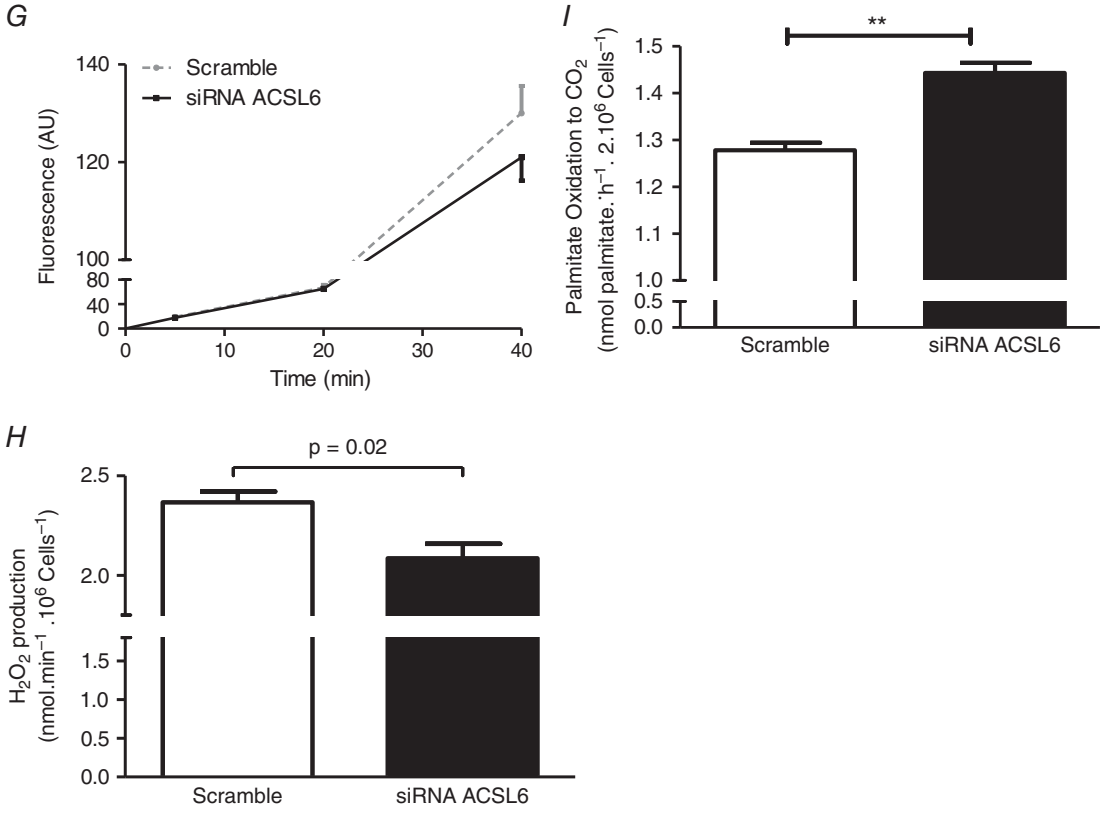

Figure 4. Continued

function of ACSL6 in skeletal muscle. In the present study, we note, under fasting and aerobic exercise conditions, a downregulation *ACSL6* mRNA. By contrast, we also demonstrate that acute lipid ingestion promotes the upregulation of the enzyme's mRNA expression. These findings compliment previous studies employing a model of acute exercise (Li *et al.* 2015) and fasting–refeeding in rats (Maschek *et al.* 2006).

The present study in isolated skeletal muscle cells also demonstrated that ACSL6 knockdown promotes a decrease in DAG, TAG and LD contents, which was accompanied by increments in fatty acid oxidation. For comparison of ACSL6 with other isoforms, studies with knockout of ASCL1 in mouse skeletal muscle demonstrated impaired fatty acid oxidation (Li *et al.* 2015). Similarly, our results were not related to increments in *ACSL1* expression, which has been considered to partition acyl-CoA into β-oxidation in skeletal muscle (Li *et al.* 2006). By contrast, we observed a downregulation of this enzyme following ACSL6 knockdown. Collectively, our results indicate that, in the rat, ACSL6 functions to partition ACSL products toward lipid synthesis and storage. Similar knockdown studies were performed by others in primary rat hepatocytes to describe the role of ACSL3 in mediating transcriptional control of lipogenesis (Bu *et al.* 2009). Surprisingly, rats consuming a chronic HFD and obese humans exhibited reduced ACSL6 mRNA levels in skeletal muscle. It has been noted that ACSL6 is regulated by insulin because this enzyme is upregulated by insulin in rat cardiomyocytes and downregulated in hearts of streptozotocin-diabetic rats (Durgan *et al.* 2006). In the present study, we employed obese rats and humans. Thus it can be conjectured that biological circumstances that promote reduced insulin sensitivity would be associated with lower levels of ACSL6 in skeletal muscle. We did not test this possibility in skeletal muscle directly; therefore, future studies are needed to support or refute the relationship between insulin sensitivity and ACSL 6 expression and function in skeletal muscle.

In the present study, genetic inhibition of *ACSL6* was associated with a stimulated cellular respiration and mitochondrial biogenesis in rat skeletal muscle cells. We attribute these effects to the elevations in C:16 and C:18 free fatty acid contents found. These molecules can acts as ligands to peroxisome proliferator-activated receptor-α, a nuclear receptor that positively regulates expression of uncoupling proteins (Grav *et al.* 2003). In our experimental model, we found higher levels of *UCP2* and *UCP3* mRNA under ACSL6 knockdown conditions in rat cells. Uncoupling proteins can compromise the efficiency of ATP production, increasing AMP/ATP or ADP/ATP ratios, which would serve to lower cellular

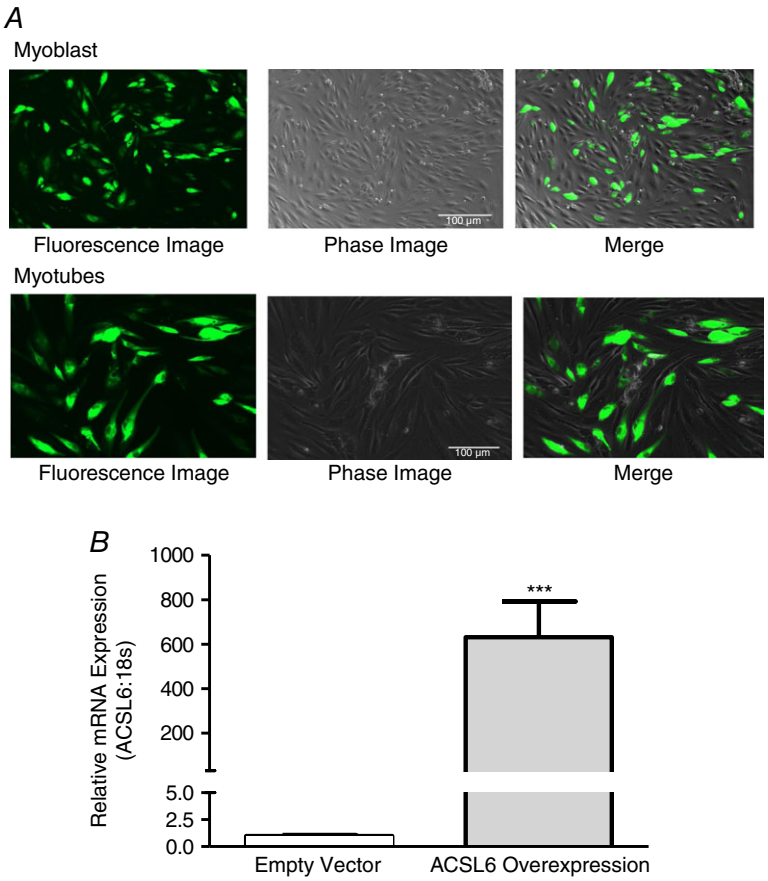

Figure 5. Efficiency of ACSL6 plasmid transfection in cells of human skeletal muscle
Representative fluorescence microscopy images of ACSL6/GFP transfection in myoblast (*A*, upper) and myotubes (*A*, lower), mRNA expression (*B*) in cells transfected with the ACSL6 plasmid or empty vector ($n = 4$ different cultures). $^{*}P < 0.05$; $^{**}P < 0.01$. [Colour figure can be viewed at wileyonlinelibrary.com]

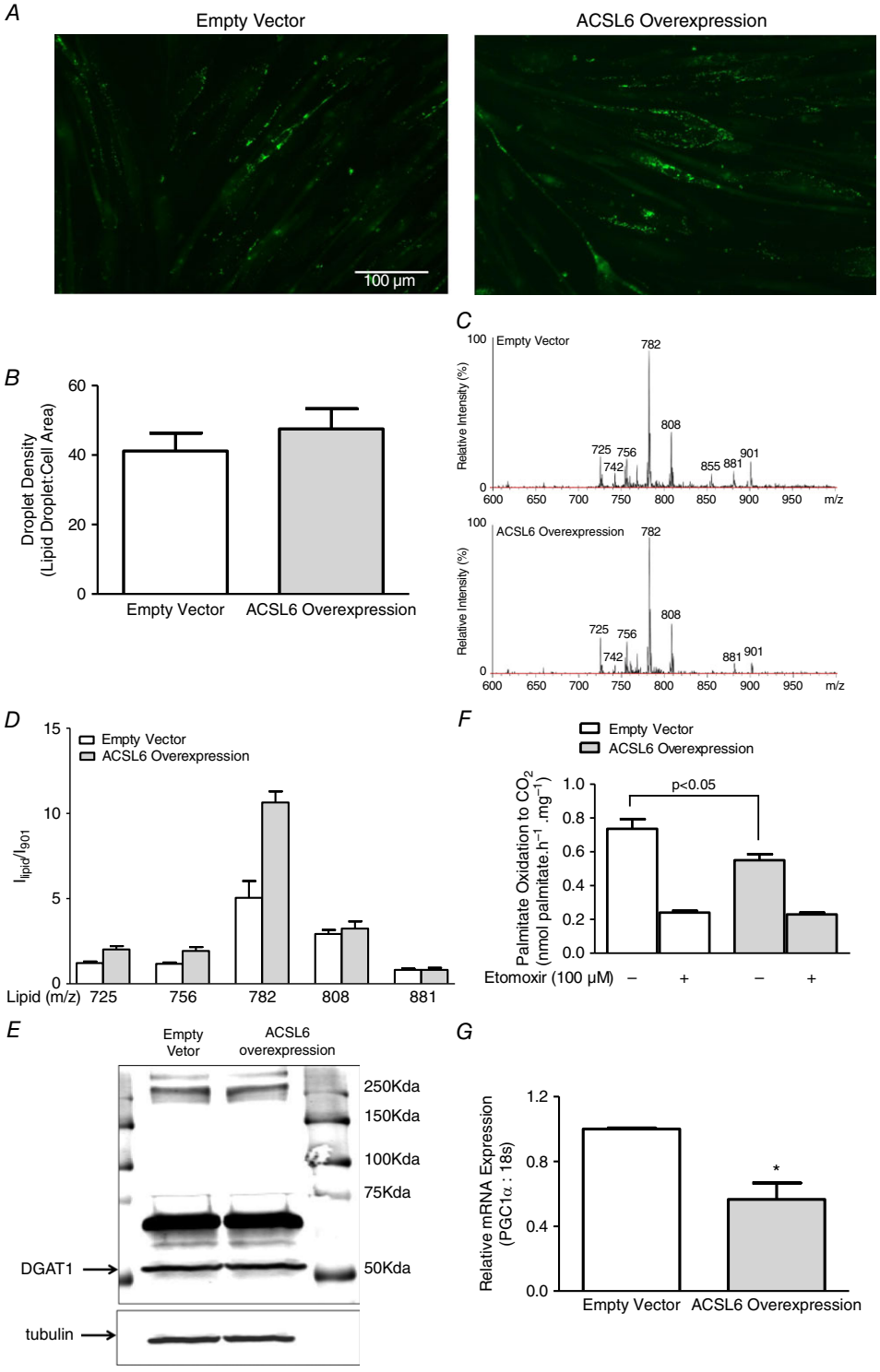

Figure 6. Effects of ACSL6 overexpression in cells of human skeletal muscle
Representative fluorescence microscopy images of LD staining using BODIPY 493/503 in empty vector (left panel) and ACSL6 transfected (right panel) cells (*A*) and LD density (*B*) ($n = 3$ independent culture and seven images of each culture), relative ion abundances of phospholipids (725:901; 756:901 and 782:901) and TAGs (808:901; 881:901) analysed by MS in empty vector (upper) and ACSL6 transfected (lower) cells (*C*) and quantification (*D*) ($n = 4$), immunoblotting of DGAT1 (*E*) ($n = 4$), radiolabelled C^{14}palmitate oxidation in the presence or not of carnitine palmitoyltransferase-1 (CPT1) inhibitor etomoxir (*F*) ($n = 6$), and PGC1α mRNA expression (*G*) ($n = 4$) in empty vector and ACSL6 transfected cells. $^{*}P < 0.05$; $^{**}P < 0.01$. [Colour figure can be viewed at wileyonlinelibrary.com]

energy charge. This alteration in the cellular bioenergetic state would lead to activation of AMPK (Hardie, 2014) as we demonstrated in the present study by elevations in the p-AMPK/AMPK. Activated-AMPK would serve to positively increase the gene expression of the *PGC-1α* (Lee *et al.* 2006), a transcriptional co-activator and master regulator of several genes of the electron transport chain, mitochondrial biogenesis, and fatty acid *β*-oxidation (Wu *et al.* 1999). The regulation of *β*-oxidation also occurs via docking and coactivation of PGC-1*α* on peroxisome proliferator-activated receptor-*α* (Vega *et al.* 2000). In support, we observed an increase in *PGC-1α* mRNA expression and higher rates of oxygen consumption determined by elevations in overall mitochondrial respiratory states (basal, leak and uncoupled respirations), which were associated with elevated rates of *β*-oxidation. Thus, the findings of the present study extend the few previous studies that have investigated the relationship between ACSL expression and mitochondrial bioenergetics/biogenesis, as previously described in hearts of mice lacking global ACSL1 expression ($ACSL^{T-/-}$) (Ellis *et al.* 2011). Given the paucity of information on the effect of ACSL6 on mitochondrial oxidative and respiratory function, further studies are warranted to understand the biological significance of ACSLs expression on cellular bioenergetics in skeletal muscle.

Consequently, we initiated these future studies and noted in ACSL6 knockdown cells, a reduction in H_2O_2 production. This observation is supported by previous reports that demonstrate a reduction in H_2O_2 production which was found to be associated with increased uncoupling protein content (Mailloux and Harper, 2011). These proteins promote a diminution in the mitochondrial membrane potential, decreasing the life-span of exposure to oxygen upstream of complex IV in the respiratory chain, and thereby reducing superoxide formation (Boveris *et al.* 1972; St-Pierre *et al.* 2002). Superoxide anion is subsequently converted to H_2O_2 by the metal-dependent enzyme superoxide dismutase. Although these species work as signalling molecules, under pathological conditions, they cause oxidative damage (Figueira *et al.* 2013). Therefore, elevated uncoupling protein expression induced by ACSL6 knockdown could protect the cell against oxidative damage by attenuating a rise in the electron transport chain proton motive force ($\Delta\Psi$) shown to result in elevations of H_2O_2 in the obese, high-fat fed and insulin resistant condition (Anderson *et al.* 2009).

In conclusion, we report for the first time a role for ACSL6 in skeletal muscle lipid metabolism. Unlike ACSL1 and ACSL4 that are associated with partitioning lipids toward mitochondrial uptake and *β*-oxidation, ACSL6 appears to drive acyl-CoA toward lipid synthesis, avoiding its oxidation in mitochondria. Moreover, ACSL6 is also involved in the modulation of cellular respiration, H_2O_2 production, lipid oxidation and mitochondrial biogenesis, which appears to involve the activation of an AMPK/PGC1-*α* pathway (Fig. 7).

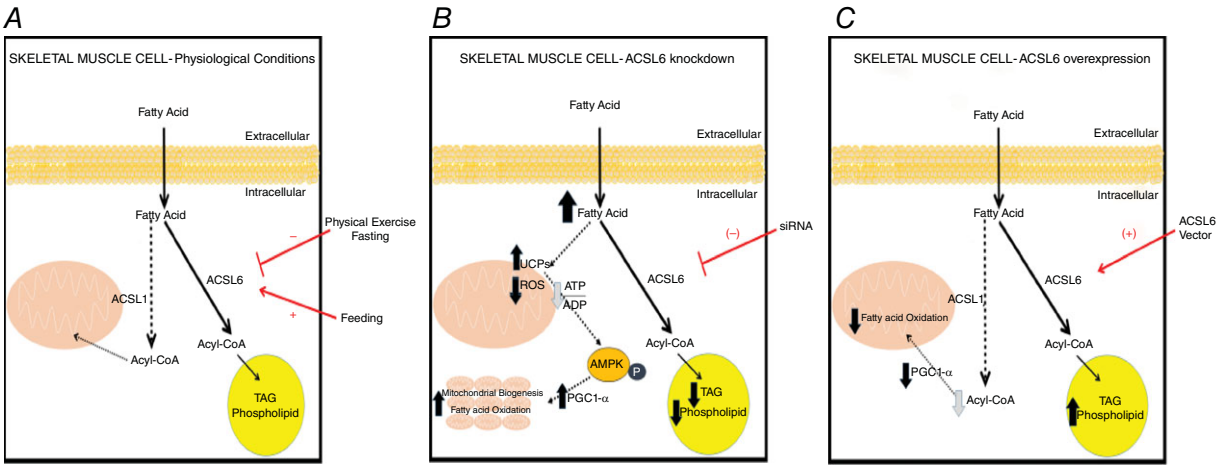

Figure 7. Representative diagram of ACSL6 mechanism
Under physiological conditions (*A*), ACSL1 drives acyl-CoA to fatty acid oxidation (Li *et al.* 2015). We propose that ACSL6 drives acyl-CoA toward lipid synthesis because physical exercise or fasting decreased mRNA ACSL6, whereas feeding increased its expression. Under ACSL6 knockdown (*B*), an increased content of free fatty acid could induce UCP expression. UCP activity could reduce ATP/ADP, resulting in the increased AMPK activation, which in turn increases mitochondrial biogenesis and fatty acid oxidation through PGC1*α*. Under ACSL6 overexpression (*C*), ACSL6 drives acyl-CoA away from mitochondria, increasing phospholipid synthesis and decreasing PGC1*α* expression and fatty acid oxidation. Black arrows indicating an increase (↑) or decrease (↓) evaluated in the present study, whereas grey arrows indicate the proposed mechanisms. [Colour figure can be viewed at wileyonlinelibrary.com]

References

Adamo KB, Dent R, Langefeld CD, Cox M, Williams K, Carrick KM, Stuart JS, Sundseth SS, Harper ME, McPherson R & Tesson F (2007). Peroxisome proliferator-activated receptor gamma 2 and acyl-CoA synthetase 5 polymorphisms influence diet response. *Obesity (Silver Spring)* **15**, 1068–1075.

Alberici LC, Oliveira HC, Catharino RR, Vercesi AE, Eberlin MN & Alberici RM (2011). Distinct hepatic lipid profile of hypertriglyceridemic mice determined by easy ambient sonic-spray ionization mass spectrometry. *Anal Bioanal Chem* **401**, 1651–1659.

Anderson EJ, Lustig ME, Boyle KE, Woodlief TL, Kane DA, Lin CT, Price JW, Kang L, Rabinovitch PS, Szeto HH, Houmard JA, Cortright RN, Wasserman DH & Neufer PD (2009). Mitochondrial H_2O_2 emission and cellular redox state link excess fat intake to insulin resistance in both rodents and humans. *J Clin Invest* **119**, 573–578.

Bharadwaj MS, Tyrrell DJ, Leng I, Demons JL, Lyles MF, Carr JJ, Nicklas BJ & Molina AJ (2015). Relationships between mitochondrial content and bioenergetics with obesity, body composition and fat distribution in healthy older adults. *BMC Obesity* **2**, 01–11.

Bizeau ME, MacLean PS, Johnson GC & Wei Y (2003). Skeletal muscle sterol regulatory element binding protein-1c decreases with food deprivation and increases with feeding in rats. *J Nutr* **133**, 1787–1792.

Bosma M (2016). Lipid droplet dynamics in skeletal muscle. *Exp Cell Res.* **340**, 180–186.

Bosma M, Kersten S, Hesselink MK & Schrauwen P (2012). Re-evaluating lipotoxic triggers in skeletal muscle: relating intramyocellular lipid metabolism to insulin sensitivity. *Prog Lipid Res* **51**, 36–49.

Boveris A, Oshino N & Chance B (1972). The cellular production of hydrogen peroxide. *Biochem J* **128**, 617–630.

Brügger B, Erben G, Sandhoff R, Wieland FT & Lehmann WD (1997). Quantitative analysis of biological membrane lipids at the low picomole level by nano-electrospray ionization tandem mass spectrometry. *Proc Natl Acad Sci USA* **94**, 2339–2344.

Bu SY, Mashek MT & Mashek DG (2009). Suppression of long chain acyl-CoA synthetase 3 decreases hepatic de novo fatty acid synthesis through decreased transcriptional activity. *J Biol Chem* **284**, 30474–30483.

Cao A, Li H, Zhou Y, Wu M & Liu J (2010). Long chain acyl-CoA synthetase-3 is a molecular target for peroxisome proliferator-activated receptor delta in HepG2 hepatoma cells. *J Biol Chem* **285**, 16664–16674.

Cases S, Smith SJ, Zheng YW, Myers HM, Lear SR, Sande E, Novak S, Collins C, Welch CB, Lusis AJ, Erickson SK & Farese RV Jr (1998). Identification of a gene encoding an acyl CoA:diacylglycerol acyltransferase, a key enzyme in triacylglycerol synthesis. *Proc Natl Acad Sci USA* **95**, 13018–13023.

Castedo M, Ferri K, Roumier T, Métivier D, Zamzami N & Kroemer G (2002). Quantitation of mitochondrial alterations associated with apoptosis. *J Immunol Methods* **265**, 39–47.

Chen J, Brunzell DH, Jackson K, Van der Vaart A, Ma JZ, Payne TJ, Sherva R, Farrer LA, Gejman P, Levinson DF, Holmans P, Aggen SH, Damaj I, Kuo PH, Webb BT, Anton R, Kranzler HR, Gelernter J, Li MD, Kendler KS & Chen X (2011). ACSL6 is associated with the number of cigarettes smoked and its expression is altered by chronic nicotine exposure. *PloS ONE* **6**, e28790.

Coleman RA, Lewin TM, Van Horn CG & Gonzalez-Baró MR (2002). Do long-chain acyl-CoA synthetases regulate fatty acid entry into synthetic versus degradative pathways? *J Nutr* **132**, 2123–2126.

Cortright RN, Sandhoff KM, Basilio JL, Berggren JR, Hickner RC, Hulver MW, Dohm GL & Houmard JA (2006). Skeletal muscle fat oxidation is increased in African American and white women after 10-days of endurance exercise training. *Obesity* **14**, 1201–1210.

Durgan DJ, Smith JK, Hotze MA, Egbejimi O, Cuthbert KD, Zaha VG, Dyck JR, Abel ED & Young ME (2006). Distinct transcriptional regulation of long-chain acyl-CoA synthetase isoforms and cytosolic thioesterase 1 in the rodent heart by fatty acids and insulin. *Am J Physiol Heart Circ Physiol* **290**, H2480–H2497.

Eberlé D, Hegarty B, Bossard P, Ferré P & Foufelle F (2004). SREBP transcription factors: master regulators of lipid homeostasis. *Biochimie* **86**, 839–848.

Ellis JM, Mentock SM, Depetrillo MA, Koves TR, Sen S, Watkins SM, Muoio DM, Cline GW, Taegtmeyer H, Shulman GI, Willis MS & Coleman RA (2011). Mouse cardiac acyl coenzyme a synthetase 1 deficiency impairs fatty acid oxidation and induces cardiac hypertrophy. *Mol Cell Biol* **31**, 1252–1262.

Fernandes AMAP, Tega DU, Jara JLP, Cunha IBS, de Sá GF, Daroda RJ, Eberlin MN & Alberici RM (2012). Free and total glycerin in biodiesel: accurate quantitation by easy ambient sonic-spray ionization mass spectrometry. *Energy Fuels* **26**, 3042–3047.

Figueira TR, Barros MH, Camargo AA, Castilho RF, Ferreira JC, Kowaltowski AJ, Sluse FE, Souza-Pinto NC & Vercesi AE (2013). Mitochondria as a source of reactive oxygen and nitrogen species: from molecular mechanisms to human health. *Antioxid Redox Signal.* **18**, 2029–2074.

Fujimura T, Takahashi S, Urano T, Takayama K, Sugihara T, Obinata D, Yamada Y, Kumagai J, Kume H, Ouchi Y, Inoue S & Homma Y (2014). Expression of androgen and estrogen signaling components and stem cell markers to predict cancer progression and cancer-specific survival in patients with metastatic prostate cancer. *Clin Cancer Res* **20**, 4625–4635.

Goto-Inoue N, Manabe Y, Miyatake S, Ogino S, Morishita A, Hayasaka T, Masaki N, Setou M & Fujii NL (2012). Visualization of dynamic change in contraction-induced lipid composition in mouse skeletal muscle by matrix-assisted laser desorption/ionization imaging mass spectrometry. *Anal Bioanal Chem* **403**, 1863–1871.

Grav HJ, Tronstad KJ, Gudbrandsen OA, Berge K, Fladmark KE, Martinsen TC, Waldum H, Wergedahl H & Berge RK (2003). Changed energy state and increased mitochondrial beta-oxidation rate in liver of rats associated with lowered proton electrochemical potential and stimulated uncoupling protein 2 (UCP-2) expression: evidence for peroxisome proliferator-activated receptor-alpha independent induction of UCP-2 expression. *J Biol Chem* **278**, 30525–30533.

Haddad R, Sparrapan R & Eberlin MN (2006). Desorption sonic spray ionization for (high) voltage-free ambient mass spectrometry. *Rapid Commun Mass Spectrom* **20**, 2901–2905.

Haddad R, Sparrapan R, Kotiaho T & Eberlin MN (2008). Easy ambient sonic-spray ionization-membrane interface mass spectrometry for direct analysis of solution constituents. *Anal Chem* **80**, 898–903.

Hardie DG (2014). AMPK: positive and negative regulation, and its role in whole-body energy homeostasis. *Curr Opin Cell Biol* **33**, C1–C7.

Heimerl S, Moehle C, Zahn A, Boettcher A, Stremmel W, Langmann T & Schmitz G (2006). Alterations in intestinal fatty acid metabolism in inflammatory bowel disease. *Biochim Biophys Acta* **1762**, 341–350.

Houmard JA, Hortobágyi T, Neufer PD, Johns RA, Fraser DD, Israel RG & Dohm GL (1993). Training cessation does not alter Glut-4 protein levels in human skeletal muscle. *J Appl Physiol* **74**, 776–781.

Kane DA, Lin CT, Anderson EJ, Kwak HB, Cox JH, Brophy PM, Hickner RC, Neufer PD & Cortright RN (2011). Progesterone increases skeletal muscle mitochondrial H_2O_2 emission in nonmenopausal women. *Am J Physiol Endocrinol Metab* **300**, E528–E535.

Lee WJ, Kim M, Park HS, Kim HS, Jeon MJ, Oh KS, Koh EH, Won JC, Kim MS, Oh GT, Yoon M, Lee KU & Park JY (2006). AMPK activation increases fatty acid oxidation in skeletal muscle by activating PPARalpha and PGC-1. *Biochem Biophys Res Commun* **340**, 291–295.

Lewin TM, Kim JH, Granger DA, Vance JE & Coleman RA (2001). Acyl-CoA synthetase isoforms 1, 4, and 5 are present in different subcellular membranes in rat liver and can be inhibited independently. *J Biol Chem* **276**, 24674–24679.

Li LO, Ellis JM, Paich HA, Wang S, Gong N, Altshuller G, Thresher RJ, Koves TR, Watkins SM, Muoio DM, Cline GW, Shulman GI & Coleman RA (2009). Liver-specific loss of long chain acyl-CoA synthetase-1 decreases triacylglycerol synthesis and beta-oxidation and alters phospholipid fatty acid composition. *J Biol Chem* **284**, 27816–27826.

Li LO, Grevengoed TJ, Paul DS, Ilkayeva O, Koves TR, Pascual F, Newgard CB, Muoio DM & Coleman RA (2015). Compartmentalized acyl-CoA metabolism in skeletal muscle regulates systemic glucose homeostasis. *Diabetes* **64**, 23–35.

Livak KJ & Schmittgen TD (2001). Analysis of relative gene expression data using real-time quantitative PCR and the 2(-Delta Delta C(T)) Method. *Methods* **25**, 402–408.

Lynge J, Juel C & Hellsten Y (2001). Extracellular formation and uptake of adenosine during skeletal muscle contraction in the rat: role of adenosine transporters. *J Physiol* **537**, 597–605.

Magnusson Y, Friberg P, Sjövall P, Dangardt F, Malmberg P & Chen Y (2008). Lipid imaging of human skeletal muscle using TOF-SIMS with bismuth cluster ion as a primary ion source. *Clin Physiol Funct Imaging* **28**, 202–209.

Mailloux RJ & Harper ME (2011). Uncoupling proteins and the control of mitochondrial reactive oxygen species production. *Free Radic Biol Med* **51**, 1106–1115.

Marszalek JR, Kitidis C, Dirusso CC & Lodish HF (2005). Long-chain acyl-CoA synthetase 6 preferentially promotes DHA metabolism. *J Biol Chem* **280**, 10817–10826.

Martin SJ, Reutelingsperger CP, McGahon AJ, Rader JA, van Schie RC, LaFace DM & Green DR (1995). Early redistribution of plasma membrane phosphatidylserine is a general feature of apoptosis regardless of the initiating stimulus: inhibition by overexpression of Bcl-2 and Abl. *J Exp Med* **182**, 1545–1556.

Mashek DG, Li LO & Coleman RA (2006). Rat long-chain acyl-CoA synthetase mRNA, protein, and activity vary in tissue distribution and in response to diet. *J Lipid Res* **47**, 2004–2010.

Parkes HA, Preston E, Wilks D, Ballesteros M, Carpenter L, Wood L, Kraegen EW, Furler SM & Cooney GJ (2006). Overexpression of acyl-CoA synthetase-1 increases lipid deposition in hepatic (HepG2) cells and rodent liver in vivo. *Am J Physiol Endocrinol Metab* **291**, E737–E744.

Privette JD, Hickner RC, Macdonald KG, Pories WJ & Barakat HA (2003). Fatty acid oxidation by skeletal muscle homogenates from morbidly obese black and white American women. *Metabolism* **52**, 735–738.

Siu PM, Donley DA, Bryner RW & Always SE (2003). Citrate synthase expression and enzyme activity after endurance training in cardiac and skeletal muscles. *J Appl Physiol* **94**, 555–560.

Soupene E, Dinh NP, Siliakus M & Kuypers FA (2010). Activity of the acyl-CoA synthetase ACSL6 isoforms: role of the fatty acid Gate-domains. *BMC Biochem* **11**, 18.

Srere PA (1969). Citrate synthase. *Method Enzymol* **13**, 3–5.

St-Pierre J, Buckingham JA, Roebuck SJ & Brand MD (2002). Topology of superoxide production from different sites in the mitochondrial electron transport chain. *J Biol Chem* **277**, 44784–44790.

Teodoro BG, Baraldi FG, Sampaio IH, Bomfim LH, Queiroz AL, Passos MA, Carneiro EM, Alberici LC, Gomis R, Amaral FG, Cipolla-Neto J, Araújo MB, Lima T, Akira US, Silveira LR & Vieira E (2014). Melatonin prevents mitochondrial dysfunction and insulin resistance in rat skeletal muscle. *J Pineal Res* **57**, 155–167.

Van Horn CG, Caviglia JM, Li LO, Wang S, Granger DA & Coleman RA (2005). Characterization of recombinant long-chain rat acyl-CoA synthetase isoforms 3 and 6: identification of a novel variant of isoform 6. *Biochemistry* **44**, 1635–1642.

Vega RB, Huss JM & Kelly DP (2000). The coactivator PGC-1 cooperates with peroxisome proliferator-activated receptor in transcriptional control of nuclear genes encoding mitochondrial fatty acid oxidation enzymes. *Mol Cell Biol* **20**, 1868–1876

Wu M, Cao A, Dong B & Liu J (2011). Reduction of serum free fatty acids and triglycerides by liver-targeted expression of long chain acyl-CoA synthetase 3. *Int J Mol Med* **27**, 655–662.

Wu Z, Puigserver P, Andersson U, Zhang C, Adelmant G, Mootha V, Troy A, Cinti S, Lowell B, Scarpulla RC & Spiegelman BM (1999). Mechanisms controlling mitochondrial biogenesis and respiration through the thermogenic coactivator PGC-1. *Cell* **98**, 115–124.

Yan S, Yang XF, Liu HL, Fu N, Ouyang Y & Qing K (2015). Long-chain acyl-CoA synthetase in fatty acid metabolism involved in liver and other diseases: an update. *World J Gastroenterol* **21**, 3492–3498.

Additional information

Competing interests

The authors declare that they have no competing interests.

Author contributions

BGT conducted most of the experiments, analysed the results and wrote part of the paper. IHS and LHMB conducted the isolation of rat cells and ACSL6 siRNA transfection, as well as some of the experiments regarding H_2O_2 production. ALQ conducted some of ACSL6 siRNA transfection and p-AMPK WB experiments. LRS design the experiments using rat cells. AOS conducted the citrate synthase activity experiments. AMAPF and MNE carried out the lipid mass spectrometry. TH and BGT conducted all of the experiments with human cells and tissue. DZ and PDN designed most of the experiments with human cells and tissue. RNC conceived the idea of the experimental design of human experiments and wrote part of the paper. LCA conceived the idea of the project, analysed all the results and wrote the paper. All authors have approved the final version of the manuscript and agree to be accountable for all aspects of the work. All persons designated as authors qualify for authorship, and all those who qualify for authorship are listed.

Funding

This study was funded by the Fundação de Amparo à Pesquisa do Estado de São Paulo (FAPESP – 2010/17259-9) and in part by National Institute of Health (NIH RO1 DK075880 – RNC, NIH R01 DK096907 – PDN). Teodoro BG was a CAPES scholarship fellow (Process Number: 99999.008343/2014-04).